

# PHYSICAL DETERMINATION OF PERMEABILITY VARIATION WITH POROSITY FOR COMPOSITE PERFORMS

**Hossein Golestanian**

**Abstract:** *This paper presents the results of experimental determination of fiber bed permeability variation with porosity. Flow measurement experiments were designed to measure fiber mat permeability for fiber beds with various fiber volume fractions. Woven fiberglass, chopped fiberglass, and carbon fiber mats were used as reinforcements. The effects of reinforcement type and porosity on fiber bed permeability were investigated. Fiber mat permeability of woven mats showed large degrees of anisotropy, whereas chopped fiberglass mats had isotropic permeability. In all cases permeability increased with fiber bed porosity. Fiber mat permeability of woven carbon was found to be about four times lower than that of woven fiberglass mats at the same porosity. This lower permeability results in longer injection time and higher manufacturing cost for composite parts made with carbon fiber mats. The results of this investigation could be employed in process/product optimization in Resin Transfer Molding (RTM) processes.*

**Keywords:** *Permeability, Porosity, Resin Flow, Carbon Mat, Fiberglass Mat*

## 1. Introduction

Resin Transfer Molding (RTM) involves transfer of resin into an enclosed mold containing previously positioned reinforcement performs. This process can be employed to manufacture large and complicated composite parts. Typical examples of products that are produced with RTM include fiberglass boats, swimming pools, bathtubs, and parts in automotive and aircraft industries [1, 2]. The reinforcement is composed of several layers of fiber mats laid inside a two-piece mold.

The mold is closed and resin is injected into the mold through one or multiple injection ports to impregnate the fibers of the perform. Injection times vary from several minutes to several hours depending on the size of the part, fiber volume fraction, fiber type, resin viscosity, and injection pressure. Once the mold is completely filled, injection is stopped and the part is cured inside the mold. The mold filling process is carried out under low pressure, thus reducing the restrictions on the tooling equipment. Mold design is a highly labor intensive and complex operation [2].

Proper mold filling requires proper positioning of the inlets and outlets, close monitoring of mold temperature and injection pressure. If the inlet pressure or resin flow rate is set too high, fiber wash out could occur [3]. Injection time must be long enough to ensure complete fiber impregnation. Also, by proper positioning of the

injection ports, one can reduce the possibility of void formation.

Fiber mat permeability determination is an important step in mold design and process control in an RTM process.

In determination of the required injection time and pressure, one needs to determine this parameter in advance. This fiber bed property depends on the amount of voids and their orientation within the fiber bed assembly. Thus the main factors affecting permeability value are the type of fiber mat and reinforcement porosity, fiber volume fraction.

## 2. Background

Large amount of research has been performed on permeability determination and resin flow analyses in RTM processes in recent years. Golestanian et al. have modeled resin flow and cure of rectangular and irregular composite parts [2, 3]. They conducted experiments to determine fiber mat permeability for 5-harness carbon and 8-harness glass mats.

They determined these properties assuming that fiber beds were homogeneous. These investigators performed experiments only on a 0.45 fiber volume fraction perform and did not investigate the effects of fiber bed porosity on permeability. Coulter and Gucerli [4] presented the results of numerical and experimental studies of resin impregnation in a two dimensional domain. They studied resin front movement in anisotropic performs and in a mold with two regions with different permeability values.

They predicted pressure distribution and resin front locations during filling of this mold. They also present

---

*Paper first received March. 12, 2007 and in revised form Nov. 02, 2007.*

*Hossein Golestanian* is with the Department of Mechanical Engineering, University of Shahrekord, Shahrekord, Beg. of Saman, Golestanian@eng.sku.ac.ir

experimental observations on the resin front location with time. Perry et al. [5] performed a complete analysis of an RTM process. Permeability measurements were conducted on woven graphite fibers. They considered a two-dimensional mold filling case. Parnas et al. [6] performed experimental and theoretical analyses to determine flow behavior in porous media. They investigated flow in heterogeneous reinforcement structures and the possibilities of void formation as a result. By performing one dimensional flow measurement experiments, they determined permeability for several types of woven mats. Lim and Lee [7] simulated mold filling of thick rectangular composite parts.

They determined three-dimensional permeability tensor for glass fiber mats. These investigators compared their flow analysis results with experimental measurements and found up to 32% error in resin front positions in some places inside the domain.

These researchers also performed flow analysis in manufacturing of a centrifugal pump cover. Han et al. performed permeability measurements of anisotropic fiber performs with a high fiber content [8]. These investigators performed pressure measurements at four locations in the flow field to determine the permeabilities for several types of fiber performs. Choi et al. [9] used a finite element software package to determine permeability at a microscopic level.

They then developed a flow model to predict resin flow in real fiber performs.

Their model predicts the interrelationship between perform properties such as permeability, fiber packing, fiber radius, and fiber volume fraction. Babu and Pillai performed experiments on resin flow behavior into woven, stitched and braided fiber mats [10]. They used a rectangular flat mold with a resin like fluid for their experiments.

They investigated inlet pressure drop with time and did not present any resin velocity data. Luke et al. [11] performed a draping analysis for the determination of fiber mat permeability as a function of deformation. They then used their determined permeability values in numerical models for the flow analysis of a car bonnet. Sawley et al. used smoothed particle hydrodynamics in finite element models to predict flow through porous media [12].

They modeled the porous media as a network of particles between which fluid flow occurred. They performed experimental measurements and compared the results with their numerical results. They demonstrated that Darcy's law predicts flow accurately when the drift velocity is low. Chan et al. determined fiber mat permeability of anisotropic fiberglass performs experimentally [13].

These investigators also determined the effect of resin flow rate on permeability of the fiber perform. Adams and Rebenfeld [14, 15] performed theoretical and experimental investigations on fiber mat permeability of anisotropic fiber performs. They performed experiments on non-woven polyester and woven Kevlar fabric to determine permeability of these fibers.

They also investigated the effects of number of fiber mats on permeability of multilayer fiber assembly. By changing the sequence of low and high permeability layers they enhanced permeability of fiber assembly. Ahn and Seferis [16] investigated the applicability of Kozeny-Carman equation to determine permeability of fiber beds in composite manufacturing. They performed measurements on plain weave T-300 carbon fabric. Their results suggested a linear increase in permeability with fiber perform porosity. All of the above investigators modeled resin flow inside the mold as flow through porous media and employed Darcy's law in their analyses. Few have determined fiber mat permeability experimentally. Fiber mat permeability variation with porosity have not been determined experimentally for plain-weave carbon, plain-weave fiberglass, and chopped fiberglass assemblies with different porosity values. The author is the first to determine permeability variation with porosity for the three fiber types mentioned above.

### 3. Resin Flow Experiments

A series of flow measurement experiments were designed to simulate the mold filling stage of an RTM process. A rectangular mold consisting of two flat plates of Plexiglas approximately 28 x 18 x 1.0 centimeters was designed. A 24 x 14 centimeter cavity was cut inside a 0.3 centimeter thick Plexiglas plate to be used as a spacer between the top and bottom pieces of the mold. This cavity represented the rectangular mold. A series of screws were used to put the three pieces together. A picture of the mold during an experiment with chopped fiberglass mats is shown in Fig. 1. Note that resin saturated part can be seen clearly and that the resin flow is circular in this case.

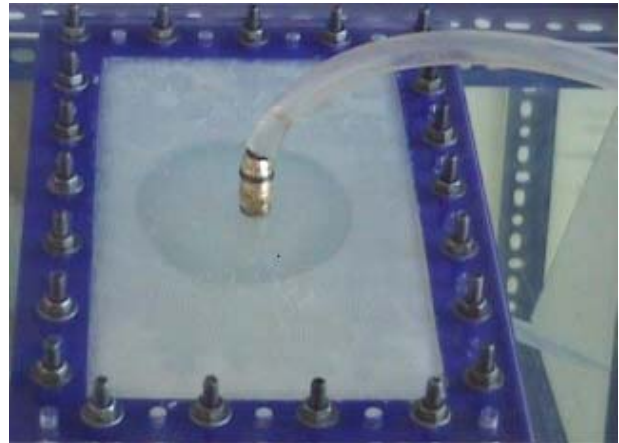


**Fig 1. A picture of the rectangular mold taken during an experiment.**

The experimental setup is shown in Fig. 2. An air pump supplies pressurized air used for the injection. The resin is put into a piece of tygon tubing connected to a pressure regulator. The injection pressure can be adjusted to the desired level and kept constant using this regulator. Resin enters the mold cavity through a central injection port devised on the top plate. A stop watch is used to keep track of elapsed time. The mold is placed on top of a 0.5 centimeter thick clear safety glass in a

four legged fixture made of dextron. Two mirrors are used to reflect the top and bottom views of the mold. A video camera, facing the mirrors, is used to record the resin flow into the mold.

RL 440 epoxy resin was used in the flow simulation experiments as the working fluid and all experiments were performed under constant injection pressure.

Several flow measurements were performed with each combination of fiber type, perform porosity, and injection pressure. A total of 40 experiments were performed on the three fiber types in the current investigation. Data analysis procedures and experimental results are presented in the next section.

#### 4. Analysis

The main objective of this study is the determination of permeability variation with fiber perform porosity. To reach our goals, a series of experiments were performed on each type of fiber mat under investigation. A video camera was used to record resin flow inside the rectangular mold cavity. Next, frames from the tapes were frozen and printed at certain time intervals.

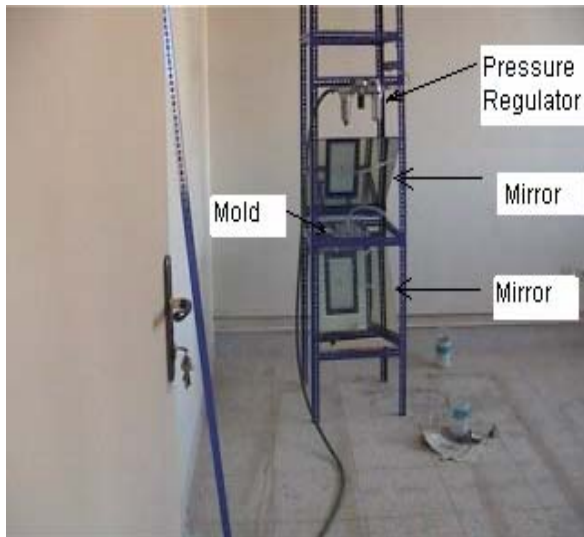


Fig 2. A picture of the designed experimental setup used for resin flow measurements.

Resin front positions were measured with time and the analysis was performed using these measurements. Based on the type of the fiber mat two types of flow were observed. Resin flow in chopped fiberglass mats was circular, suggesting a homogeneous and isotropic permeability. In the case of woven fiberglass and carbon fiber assemblies, resin front had an elliptic shape. This elliptic flow front suggests an orthotropic perform. Analysis in each case was then performed based on the resin front shape observed in the experiments. Formulations and analysis procedures for these cases are described below.

#### 4-1. Governing Equations

For the flow of an incompressible fluid through a porous medium, with negligible gravitational forces, Darcy's law reduces to [2,17];

$$v = -\frac{K}{\mu} \nabla P \quad (1)$$

In Equation (1)  $v$  is fluid velocity,  $K$  is the perform permeability tensor,  $\mu$  is the fluid viscosity, and  $\nabla P$  is pressure gradient.

#### 4-2. Analysis of Isotropic Perform

The isotropic working equation for the in-plane flow experiment is [3];

$$\frac{dR_f}{dt} = \frac{K\Delta P}{\varepsilon\mu} \frac{-1}{R_f \ln(R_f/R_o)} \quad (2)$$

Where  $\varepsilon$  is the fiber perform porosity,  $R_f$  and  $R_o$  are the radii of the moving fluid and the injection port, respectively.

The boundary condition for Equation (2) is;

$$R_f = R_o \quad \text{at } t = 0$$

The solution to Equation (2) subject to the above boundary condition is [3];

$$G(\rho_f) = [\rho_f^2 (2 \ln \rho_f - 1) + 1] / 4 = \frac{K\Delta Pt}{\varepsilon\mu R_o^2} \quad (3)$$

where  $\rho_f = R_f / R_o$  is a dimensionless radial extent. In Equation (3)  $\Delta P$  is specified experimentally and  $\varepsilon$  is known from the fibrous perform type and number of lamina. Discrete  $R_f(t)$  data may be plotted in the form of  $G(\rho_f)$  vs. time as suggested by Equation (3). Least squares line is fit through the data, and the isotropic in-plane permeability is determined from the slope of the line as [3];

$$K = \frac{m\varepsilon\mu R_o^2}{\Delta P} \quad (4)$$

Where,  $m$  is the slope of the best fit line through the data. The porosity of the stacked fiber mat layers is given by [16];

$$\varepsilon = 1 - \frac{NA_w}{\rho_f T_m} \quad (5)$$

In Equation (5)  $N$  is the number of plies,  $A_w$  is the total weight of a fabric ply,  $\rho_f$  is fiber density, and  $T_m$  is the thickness of the laminated fabric perform. The analysis involves resin front measurements with time during the injection cycle. First printouts of several frames at known elapsed times were obtained from the video tape on each experiment.

Then the resin front positions were measured and the degree of circularity was checked. Resin front in chopped fiberglass mats advanced in a circular fashion, suggesting homogeneous fiber mat permeability in this case. Then the results were plotted as  $G(\rho_f)$  vs. time and the best fit line was obtained. Using the slope of the best fit line in Equation (4), the permeability was determined for each fiber perform for three porosity values. The results of these analyses are presented in the Experimental Results section.

### 4-3. Analysis of Orthotropic Perform

Resin front advanced with an elliptic shape in the experiments with woven fiberglass and carbon fiber mats. This suggests an orthotropic permeability tensor. The analysis in this case requires a different formulation approach.

The analysis follows the formulation given by Adams and Rebenfeld [14, 15]. In this case the governing differential equation of the moving resin front is:

$$\frac{d\zeta}{dt} = \frac{k_1 \Delta P}{\varepsilon \mu R_o^2} \left[ \frac{\alpha}{1-\alpha} \right]^* \left[ \frac{1}{(\zeta_f - \zeta_o)(\cosh^2 \zeta_f - \cos^2 \eta)} \right] \quad (6)$$

In Equation (6)  $\zeta_f$  is an elliptical extent,  $\eta$  is the elliptical equivalent of the in-plane angle, and  $\alpha$  is the ratio of the permeability, given by;

$$\alpha = \frac{K_2}{K_1} \quad (7)$$

Where,  $K_1$  and  $K_2$  are the directional permeability in the directions of maximum and minimum flow, respectively. In addition,  $\zeta_o$  is the elliptical equivalent of the injection port radius given by;

$$\zeta_o = \ln \left[ \frac{1 + \alpha^{1/2}}{(1 - \alpha)^{1/2}} \right] \quad (8)$$

Subjected to the initial conditions;

$$\zeta_f = \zeta_o \quad \text{at} \quad t = 0$$

The relations between the radial and elliptical extents in these directions are given by;

$$\zeta_{f1} = \sinh^{-1} \left[ \frac{R_{f1}}{R_o} \left( \frac{1}{\alpha} - 1 \right)^{-1/2} \right] \quad (9)$$

And;

$$\zeta_{f2} = \cosh^{-1} \left[ \frac{R_{f2}}{R_o} (1 - \alpha)^{-1/2} \right] \quad (10)$$

The solution to Equation (6) is;

$$F(\zeta_f, \eta) = (\zeta_f - \zeta_o) \left( \frac{\sinh(2\zeta_f)}{4} + \frac{\zeta_f}{2} \right) + \cos^2 \eta (\zeta_f \zeta_o - (\zeta_f^2 + \zeta_o^2) / 2) + (\cosh(2\zeta_o) - \cosh(2\zeta_f)) / 8 + (\zeta_o^2 - \zeta_f^2) / 4 = \left[ \frac{\alpha}{1-\alpha} \right] \Phi \quad (11)$$

Where,  $\Phi$  is based on the maximum in-plane permeability,  $K_1$ . The anisotropic data analysis is iterative in  $\alpha$ . First  $\alpha$  is guessed and the experimental data are converted to equivalent elliptical extents and are plotted for the two data sets.

A single least squares analysis is then performed on the two sets of data. The single least squares line will not fit both sets of data properly if  $\alpha$  is not chosen correctly. By

changing  $\alpha$  and monitoring the errors, the best value for  $\alpha$  is selected.

$$m_\zeta = \frac{K_1 \Delta P}{\varepsilon \mu R_o^2} \left[ \frac{\alpha}{1-\alpha} \right] \quad (12)$$

After  $\alpha$  is selected properly, the slope of the best fit line is used in Equation (12), along with Equation (7) to determine the directional permeability values,  $K_1$  and  $K_2$ .

## 5. Results and Discussion

Analyses were performed on the experimental results of the three fiber mat types following the procedures outlined above. The results of the best fit lines are presented for selected experiments with each fiber mat type in Figs. 3 through 5. In case of chopped fiberglass mats the analysis followed the isotropic analysis procedure. The best fit line for the selected experiment on these mats is presented in Fig. 3. Note that one set of data points is measured and fitted since circular flow patterns were observed in the chopped fiberglass mats. Fig. 4 presents the results of the selected experiment on woven fiberglass mats.

The flow pattern was elliptic in this case and two sets of data points are fitted by a single best fit line as explained in the analysis section. The results of the selected experiment on woven carbon fiber mats are shown in Fig. 5. The analysis followed the orthotropic perform procedure for the carbon mats as well.

The permeability analysis was performed on several cases for each fiber type. Resin viscosity was 440 centipoises, given in the manufacturer's data sheet. In each case the effect of fiber bed porosity on perform permeability was investigated. From the results of these analyses plots of permeability vs. porosity was generated for each fiber type. Figs. 6 through 8 depict these permeability maps. Variation of perform permeability with porosity of chopped fiberglass mats is shown in Fig. 6. Note that permeability increases sharply as porosity increases to 0.84. As porosity increases, the amount of void space available to resin flow increases. Thus, resin flows more easily and faster into fiber beds with lower fiber volume fractions.

It seems that there is a more moderate increase in permeability at porosity values below 0.8. Fig. 7 depicts the variation of perform permeability with porosity for woven fiberglass mats. Resin front advanced in an elliptic shape in these mats. Thus, the analysis on these fibers followed the orthotropic perform analysis procedure and perm abilities in the directions of maximum and minimum flow are determined. Note that permeability increases with porosity for these fibers as well.

Variation of perform permeability with porosity for woven carbon mats is shown in Fig. 8. Resin flow was orthotropic in these mats as well thus the permeability tensor is anisotropic for both woven carbon and woven fiberglass mats. Note also that permeability of fiberglass mats is about four times that of carbon perform at the same porosity value. This suggests longer injection times and higher manufacturing costs for composite parts with carbon fiber mats.

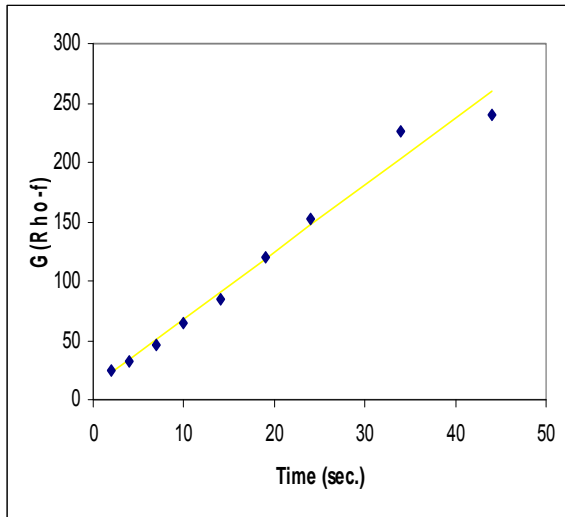


**Fig 3. The best fit line fitted through the experimental data on chopped fiberglass mats.**

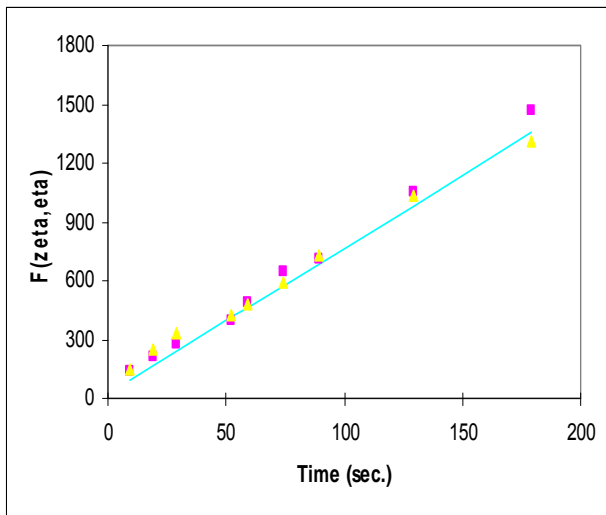


**Fig 4. The best fit line fitted through the experimental results on woven fiberglass mats.**

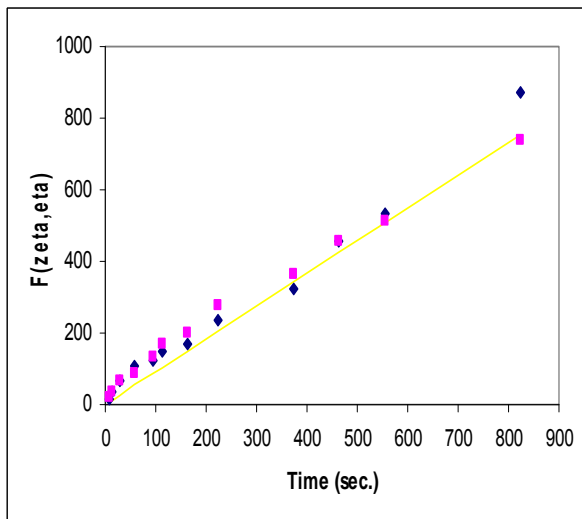


**Fig 5. The best fit line fitted through the experimental results on woven carbon mats.**

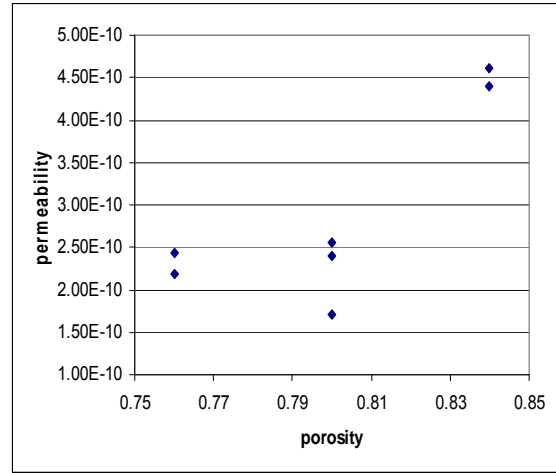


**Fig 6. Variation of perform permeability with porosity for chopped fiberglass mats**

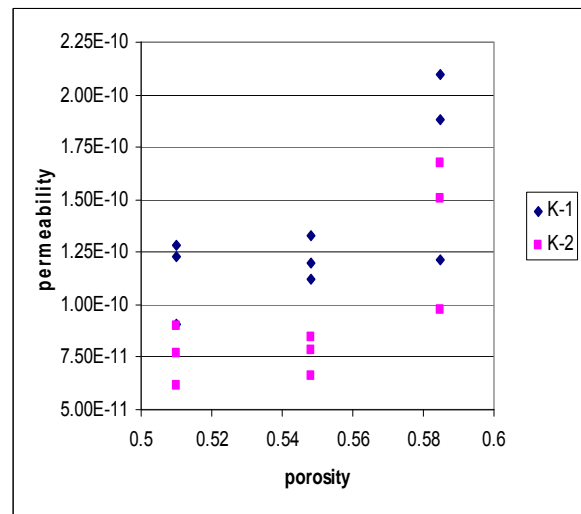


**Fig 7. Variation of perform permeability with porosity for woven fiberglass mats.**

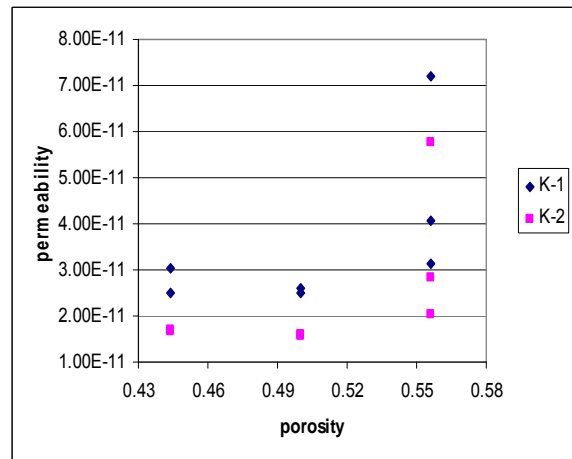


**Fig 8. Variation of perform permeability with porosity for woven carbon mats**

**6. Concluding Remarks**

Resin flow experiments were performed to determine variation of fiber bed permeability with perform porosity. Three types of fiber perform s were used in the experiments. The investigation was performed with

woven carbon mats, woven fiberglass mats, and chopped fiberglass mats. Experiments were performed at three fiber bed porosity values with each fiber type. Each experiment was performed under constant pressure conditions and RL 440 Epoxy resin was used as the working fluid. Permeability tensor for chopped fiberglass mats was found to be isotropic. In case of woven fiberglass and woven carbon mats, permeability tensor came out to be orthotropic. That is, resin flow in these mats was elliptic. In general perform permeability increases sharply as porosity increases above a certain value. This suggests a decrease in permeability with an increase in fiber volume content. This means higher injection times and, in turn, higher manufacturing costs for a part with higher fiber content in an RTM process. In addition, fiber bed permeability was measured to be much lower for carbon mats. This indicates that the injection cycle will be much longer for parts manufactured using carbon fiber mats in comparison with either chopped or woven fiberglass mats with the same porosity or fiber content.

#### Acknowledgements

The author wishes to thank the Iranian Industries and Mines Ministry and Iranian Higher Education Ministry for providing financial support for this research.

#### References

- [1] Richardson Terry, Composites, A Design Guide, Industrial Press Inc., New York 1987.
- [2] Golestanian, H., "Modeling of process induced residual stresses and resin flow behavior in resin transfer molded composites with woven fiber mats," Ph. D. thesis, Department of Mechanical and Aerospace Engineering, University of Missouri-Columbia, MO, 1997.
- [3] Golestanian, H., & El-Gizawy Sherif, A., "Physical and numerical modeling of mold filling in resin transfer molding," Polymer Composites, Vol. 19, (4), 1998, PP. 395-407.
- [4] Coulter, J.P., & Gucer, S.I., "Resin transfer molding: process review, modeling and research opportunities," Manufacturing International, Vol. IV, 1998, PP. 79-86.
- [5] Perry, M.J., Wang, T.J., Ma, Y., & Lee, L.J., "Resin transfer molding of epoxy/graphite composites," 24th International SAMPE Technical Conference, 1992, T421.
- [6] Parnas, R.S., Salem, A.J., Sadiq Thomas, A.K., Wang Hsin-Peng, & Advani, S.G., "The interaction between micro- and macro-scopic flow in RTM performs," Composite Structures, Vol. 27, 1994, PP. 93-107.
- [7] Lim, S.T., & Lee Woo, II., "An analysis of the three-dimensional resin-transfer mold filling process," Composites Science and Technology, Vol. 60, 2000, PP. 961-975.
- [8] Han, K.K., Lee, C.W., & Rice, B.P., "Measurements of the permeability of fiber performs and applications," Composites Science and Technology, Vol. 60, 2000, PP. 2435-2441.
- [9] Choi Mi Ae, Lee Mi Hye, Chang, J., & Lee, S.J., "Permeability modeling of fibrous media in composite processing," Non-Newtonian Fluid Mech., Vol. 79, 1998, PP. 585-598.
- [10] Babu, B.Z., & Pillai, K.M., "New experimental findings on resin impregnation process for woven, stitched or braided fiber mats in liquid composite molding," SAMPE Conference, Long Beach, CA, 2002.
- [11] Luca, P., Benoit, Y., & Trochon, J., "Coupled pre-forming/injection simulations of liquid composite molding processes," SAMPE Conference, Long Beach, CA, 2002.
- [12] Sawley, M.L., Cleary, P.W., & HA Joseph, "Modeling of flow through porous media and resin transfer molding using smoothed particle hydrodynamics," CSIRO, Melbourne, Australia, 1999.
- [13] Chan, A.W., Larive, D.E., & Morgan, R.J., "Anisotropic permeability of fiber performs: constant flow rate measurements," Composite Materials, Vol. 27 (10), 1993, PP. 996-1008
- [14] Adams, K.L., & Rebenfeld, L., "Permeability characteristics of multilayer fiber reinforcements. Part II: Theoretical model," Polymer Composites, Vol. 12 (3), 1991, PP. 186-190.
- [15] Adams, K.L. & Rebenfeld, L., "Permeability characteristics of multilayer fiber reinforcements. Part II: Theoretical model," Polymer Composites, Vol. 12 (3), 1991, PP. 179-185.
- [16] Ahn, K.J., & Seferis, J.C., "Simultaneous measurements of permeability and capillary pressure of thermosetting matrices in woven fabric reinforcements," Polymer Composites, Vol. 12 (3), 1991, PP. 146-152.
- [17] Bird, R.B., Stewart, W.E., & Lightfoot, E.N., Transport Phenomena, John Wiley & Sons, New York, 1960.

#### Nomenclature

$A_w$  : total weight of a fabric ply

$\underline{K}$ : permeability tensor

$K_1$ : directional permeability in the direction of maximum flow

$K_2$ : directional permeability in the direction of minimum flow

M: slope of the best fit line

N: number of plies

$R_f$ : radius of the moving fluid

$R_o$ : radius of the injection port

t: time

$T_m$ : thickness of the laminated fabric perform

v: fluid velocity

### Greek Symbols

$\alpha$ : ratio of the perm abilities

$\varepsilon$ : porosity of the fiber bed,

$\eta$ : elliptical equivalent of the in-plane angle

$\Phi$ : function based on the maximum in – plane permeability

$\mu$ : fluid viscosity

$\nabla P$ : pressure gradient

$\rho$ : fluid density,

$\rho_f$ : fiber density

$\rho_f$ : dimensionless radial extent, =  $R_f/R_o$

$\xi_o$ : elliptical equivalent of the injection port radius

$\xi_f$ : an elliptical extent